Saudi Journal of Biological Sciences 27 (2020) 3290–3300

Contents lists available at ScienceDirect

Saudi Journal of Biological Sciences

journal homepage: www.sciencedirect.com

Original article

# Caspase dependent apoptotic activity of polycyclic cage-like heterocyclic hybrids

Raju Suresh Kumar [a,*], Abdulrahman I. Almansour [a], Natarajan Arumugam [a], D. Kotresha [b], Janardhana Papayya Balakrishna [c]

[a] Department of Chemistry, College of Science, King Saud University, P.O. Box 2455, Riyadh 11451, Saudi Arabia
[b] Department of Botany, Davangere University, Shivagangothri, Davangere- 577007, Karnataka, India
[c] Department of Stem Cell Biology, Stellixir Biotech Pvt Ltd, No.V-31, 2nd Floor, 10th Main Road, Peenya 2nd Stage Industrial Area, Bangalore 560058, Karnataka, India

ARTICLE INFO

*Article history:*
Received 4 August 2020
Revised 3 September 2020
Accepted 20 September 2020
Available online 25 September 2020

*Keywords:*
Cage-like heterocyclic hybrids
HCT116
JURKAT
Apoptosis
Cell cycle
TUNEL Assay
Caspase 3

ABSTRACT

A small library of cage-like heterocyclic hybrids encompassing pyrroloisoquinolines, pyridinone and acenaphthene structural moieties have been synthesized and tested for their potential as anticancer agents against HCT116 and JURKAT cell lines. The results revealed that these cell lines are more sensitive towards compound **1g** and it showed dose dependent cytotoxic effect at 48 hrs of incubation. The $IC_{50}$ values of compound **1g** against HCT116 and JURKAT cell lines are 12.14 ± 1.53 and 10.68 ± 0.68 μM, respectively. Further studies on the determination of mechanism of action of compound **1g** discovered that it brought the cell death by inducing Caspase 3 dependent apoptosis and also by arresting the cell cycle at S phase. These studies revealed that compound **1g** can be recommended as a potential anticancer agent.



## 1. Introduction

Uncontrolled division and differentiation of cells is known as cancer. Worldwide cancer is a major cause of mortality (Ames et al., 1995). After cardiovascular diseases cancer was found second leading cause with the higher mortality rate in the United States, while great steps have been made in the treatment of cancer over the past 50 years, it remains to be a foremost health concern and, hence, broad efforts have been devoted in search of new therapeutic approaches (Stewart and Kleihues, 2014; Kanavos, 2006). Due to advances in the early detection, diagnosis and preventive treatments reduction in death rates were observed (Gralow et al., 2008). Over 100 years of the research demonstrated that the cancer could be treated effectively through various different strategies such as surgery, chemotherapy and radiotherapy. The treatment strategies when combined or applied alone can significantly affect the growth of the tumor (Wolinsky et al., 2012; Chen et al., 2016). The combination therapy can be impactful on various solid cancers such as, colon, breast etc. Once the metastasis starts in the tumor, the treatment for the specific cancer becomes more complicated (Weidner 1995). There are still most of the significant challenges remaining for various different cancer one of the widely known example is glioblastoma, in which the early detection, diagnosis, chemotherapy and even surgery results into failure to extend the lifespan and survival beyond 2 years (Grossman and Batara, 2004; Maier-Hauff et al., 2007). Colon cancer is one of the common cancers in the US and is proved to be a second largest cause of deaths. Differences in the right and left colon may be due to histological, genetic and immunological features (Lim et al., 2017; Todaro et al., 2007). Typically, colon cancer can occur at any age, it starts with the benign cancer called polyps occurs inside the colon. As time goes, the cancer becomes cancer of the colon (Todaro et al., 2007). In the development phase of the colon cancer, so many treatment strategies are available for the prevention and control. There are no prominent symptoms are noticed in the early stages of the cancer. In the progression stage, the symptoms are more noticeable (Adrouny 2002; Boyle et al., 2000).

* Corresponding author.
*E-mail address:* sraju@ksu.edu.sa (R.S. Kumar).

Peer review under responsibility of King Saud University.

Production and hosting by Elsevier

https://doi.org/10.1016/j.sjbs.2020.09.042
1319-562X/

Heterocyclic hybrids possessing Nitrogen are prevalent in myriad natural products and used as honored structures in small molecules (Gomtsyan, 2012; Eicher et al., 2012). Among diverse biologically potent alkaloids, pyrroloisoquinoline structural units are common and present in lycorine class of Amaryllidaceae alkaloids (Eicher et al., 2012; Nair et al., 2016) and phenanthroindolizidine alkaloids (Pereira et al., 2015) besides, these structural subunits are also prevalent in Crispine A (Zhang et al., 2002), Harmicine (Kam and Sim, 1998; Chakraborty and Jana, 2013), Erysotramidine and Lamellarins (Andreev et al., 2016) displaying valuable therapeutic properties. Furthermore, some synthetic derivatives possessing this heterocyclic subunit also showed potential pharmacological properties (Sorgi et al., 1990). Research studies on anticancer drugs discloses that pyridinone derivatives with an α,β-unsaturated carbonyl group shown fluorescent properties emphasizing their potential as theranostic agents and displayed effective activity against cancer cell lines. In particular, 3,5-bis(arylidene)-4-piperidones reveal low-micromolar to sub-micromolar $IC_{50}$ values towards a number of cancer cell lines (Sorgi et al., 1990; Santiago-Vazquez et al., 2014). Acenaphthopyrrole derivatives also displayed sub-micromolar activity against specific cancer cell lines (Liu et al., 2006; Zhang et al., 2006). Consequently, the heterocyclic hybrids comprising pyrrolo[1,2-b] isoquinolines, pyridinone and acenaphthene structural sub units could be valuable in forthcoming studies for drug development. Contemplations on the anticancer drugs led us to focus our research on novel anticancer agents with high selectivity and diminished toxicity. In our recent study (Kumar et al., 2020), we explored the synthesis and anticancer evaluation of a cage-like heterocyclic hybrid derived from a dipolarophile with phenyl groups. In the present study, we reported the apoptotic inducing ability of cage-like heterocyclic hybrids possessing different substituted aryl rings, biologically active pyrroloisoquinoline, pyridinone and acenaphthene structural moieties.

## 2. Materials and methods

### 2.1. Chemistry

Melting points of the cage compounds were determined by open capillary tubes and are uncorrected. $^1H$ and $^{13}C$ Nuclear Magnetic Spectra (NMR) were documented on a Bruker 500 MHz instrument in $CDCl_3$ using Tetramethylsilane (TMS) as internal standard and standard Bruker software was used. IR spectra of the cage compounds were recorded on a Perkin Elmer system 2000 FT-IR (KBr). Elemental analyses were performed on a Perkin Elmer 2400 Series II Elemental CHNS analyzer.

#### 2.1.1. Cage-like heterocyclic hybrid **1g**

Pale brown solid, (90%); mp = 189–191 °C; IR (KBr): 1597, 1685, 3426 $cm^{-1}$; $^1H$ NMR (500 MHz, $CDCl_3$): $\delta_H$ 2.83 (1H, dd, *J* = 14.0, 8.5 Hz, H-18), 2.98 (1H, d, *J* = 12.0 Hz, H-25), 3.05 (1H, dd, *J* = 14.5, 5.0 Hz, H-18), 3.21 (1H, d, *J* = 14.0 Hz, H-13), 3.32 (1H, d, *J* = 16.5 Hz, H-24), 3.57–3.64 (2H, m, H-13 and H-24), 4.22–4.24 (2H, m, H-20 and H-25), 4.39–4.42 (1H, m, H-19), 6.17 (1H, s, H-26), 6.32 (2H, d, *J* = 8.5 Hz, ArH), 6.71 (1H, d, *J* = 7.0 Hz, ArH), 7.02 (1H, d, *J* = 7.0 Hz, ArH), 7.05 (2H, d, *J* = 8.5 Hz, ArH), 7.10–7.12 (1H, m, ArH), 7.16 (1H, d, *J* = 7.5 Hz, ArH), 7.21 (1H, d, *J* = 7.0 Hz, ArH) 7.28–7.38 (3H, m, ArH), 7.45–7.48 (2H, m, ArH), 7.55 (1H, d, *J* = 8.5 Hz, ArH), 7.60 (1H, d, *J* = 7.0 Hz, ArH), 7.71 (2H, d, *J* = 8.5 Hz, ArH). $^{13}C$ NMR (125 MHz, $CDCl_3$): $\delta_C$ 34.31, 47.93, 51.72, 52.85, 56.33, 63.02, 72.66, 94.43, 121.20, 124.31,125.85, 125.95, 126.37, 126.53, 127.40, 127.50, 127.65, 128.08, 128.78, 128.85, 130.27, 130.74, 131.66, 132.22, 133.29, 133.56, 134.30, 134.43, 134.77, 135.15, 135.18, 135.35, 136.61, 136.76, 138.38, 196.51. Anal. calcd for $C_{40}H_{30}Cl_2N_2O_2$: C, 74.88; H, 4.71; N, 4.37%; found: C, 74.69; H, 4.83; N, 4.51%.

### 2.2. Biology

Cell lines (HCT116, JURKAT) were obtained from ATCC (American Type Culture Collection) situated in Virginia, USA. D-MEM (cat no. AL111), Fetal Bovine Serum (cat no. RM10432), D-PBS (cat no. TL1006) was purchased from Himedia, Camptothecin (Cat No: C9911) was procured from Sigma Alddrich, India, Propidium Iodide (cat 556463); APO-DIRECT™ Kit (cat no. 556381); FITC Rabbit Anti- Active Caspase-3 (cat no. 560901); FITC Annexin V Apoptosis Detection Kit I (cat no. 556547); MitoScreen Kit-JC-1 (cat No. 551302) were collectively purchased from BD biosciences.

#### 2.2.1. Cell line and cell culture

The HCT116 and JURKAT cell lines were obtained from ATCC (American Type Culture Collection) situated in Virginia, USA. The cell line were grown in Dulbecco's Modified Eagle's Medium (DMEM) and for enhancement for growth addition with 10% of fetal bovine serum, 100 $\mu g \cdot mL^{-1}$ of streptomycin, 100 $UI \cdot mL^{-1}$ of penicillin and the cultures were being maintained at 37 °C within a humidified air atmosphere with 5% (V/V) $CO_2$.

#### 2.2.2. Maintenance of cell line

The vial containing the HCT-116 and JURKAT cell lines acquired from ATCC was taken from liquid nitrogen freezer and immediately placed in a 37 °C water bath. It was whirled until a small ice crystal remained. The entire content was transferred into a 15 mL centrifuge tube. Later the cryopreservation medium was removed by centrifuging for 10 min at 2000 RPM, at room temperature. Then the cell pellet was washed with fresh cell culture medium to remove residual DMSO. The cells were maintained in a T25 flask at recommended density and once 80% confluency was reached, the cells were sub-cultivated in 1:4 ratio.

#### 2.2.3. Apoptosis assay

Annexin V/FITC Kit (BD Biosciences, Catalogue no. 556547), was used for performance of apoptosis assay and the fluorescence intensities of annexin-V-FITC and PI in drug treated and control cells were estimated by using flow cytometer. One million of HCT-116 cells were seeded in required number of wells of a 6-well plate and cultured for 12 hrs. Later, the spent medium was removed and cells were cultured in medium containing test compounds at $IC_{50}$ value for 48 hrs. After incubation, the cells were collected by trypsinization and washed twice with PBS. The cells were resuspended in 100 μL of annexin V-FITC binding buffer (1×) and 5 μL annexin V-FITC and incubated in the dark for 10 min at 25 °C. The cells were then washed with PBS by centrifugation at 2000 rpm for 5 min. The cell pellet was resuspended in 500 μL annexin V-FITC binding buffer (1×) and 5 μL PI, followed by flow cytometric analysis.

#### 2.2.4. Assessment of mitochondrial membrane potential ($\Delta\Psi$ m)

$1 \times 10^6$ HCT-116 cells/well were seeded in a 6-well plate and cultured for overnight. After adherence to the plastic surface, the cells were incubated in medium containing compound **1g** and CPT at their $IC_{50}$ values for 48 hrs. The spent medium was discarded and the cells were harvested by trypsinization and PBS wash. 70% ice-cold ethanol was used to fix the cells by incubating at −20 °C for 30 min. Then, 0.5 mL of freshly prepared JC-1 solution was added to each cell pellet and incubated for 10–15 min at 37 °C in a $CO_2$ incubator. 1 mL of assay buffer was used to wash the cells and then resuspended the cell pellets in 0.5 mL of assay buffer. Mitochondrial membrane potential ($\Delta\Psi$ m) was determined by BD FACS Calibur.

*2.2.5. Caspase 3 expression studies:*

6-well plate was used for seeding of HCT-116 cells ($1 \times 10^6$ cells/well). After overnight culture at 37 °C in a $CO_2$ incubator, the spent medium was replaced with culture medium containing compound **1g** and CPT at $IC_{50}$ values and incubated for 48 hrs. Cells were collected by trypsinization and harvested by thorough PBS wash. 70% ice cold ethanol was applied to fix and permeabilize the cells by incubating at −20 °C temperature for 30 min. After, PBS wash the cells were incubated with 20 μL of Caspase 3 -FITC for 1 hr. at RT in dark. The cells were washed with PBS to remove unbound antibodies and resuspended in 0.5 mL of PBS. The Caspase3 expression was determined by BD FACS Calibur.

*2.2.6. Cell cycle analysis*

Initially HCT-116 cells ($1 \times 10^6$ cells/well) were seeded in a 6-well plate and cultured for overnight and then exposed to

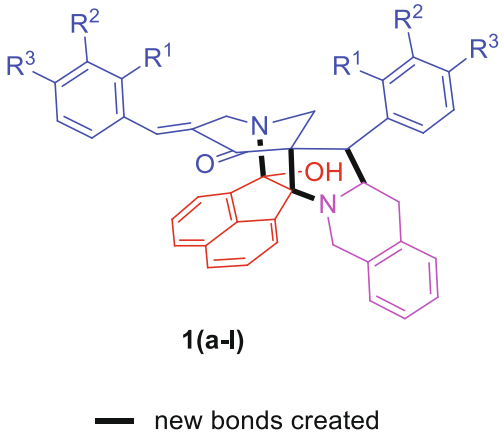


**1a**: $R^1 = CH_3$; $R^2 = H$; $R^3 = H$
**1b**: $R^1 = H$; $R^2 = H$; $R^3 = CH_3$
**1c**: $R^1 = OCH_3$; $R^2 = H$; $R^3 = H$
**1d**: $R^1 = H$; $R^2 = OCH_3$; $R^3 = H$
**1e**: $R^1 = H$; $R^2 = H$; $R^3 = OCH_3$
**1f**: $R^1 = Cl$; $R^2 = H$; $R^3 = H$
**1g**: $R^1 = H$; $R^2 = H$; $R^3 = Cl$
**1h**: $R^1 = H$; $R^2 = Cl$; $R^3 = Cl$
**1i**: $R^1 = Br$; $R^2 = H$; $R^3 = H$
**1j**: $R^1 = F$; $R^2 = H$; $R^3 = H$
**1k**: $R^1 = H$; $R^2 = Cl$; $R^3 = F$
**1l**: $R^1 = H$; $R^2 = NO_2$; $R^3 = H$

**Scheme 1.** Cage-like heterocyclic hybrids **1**(**a-l**).

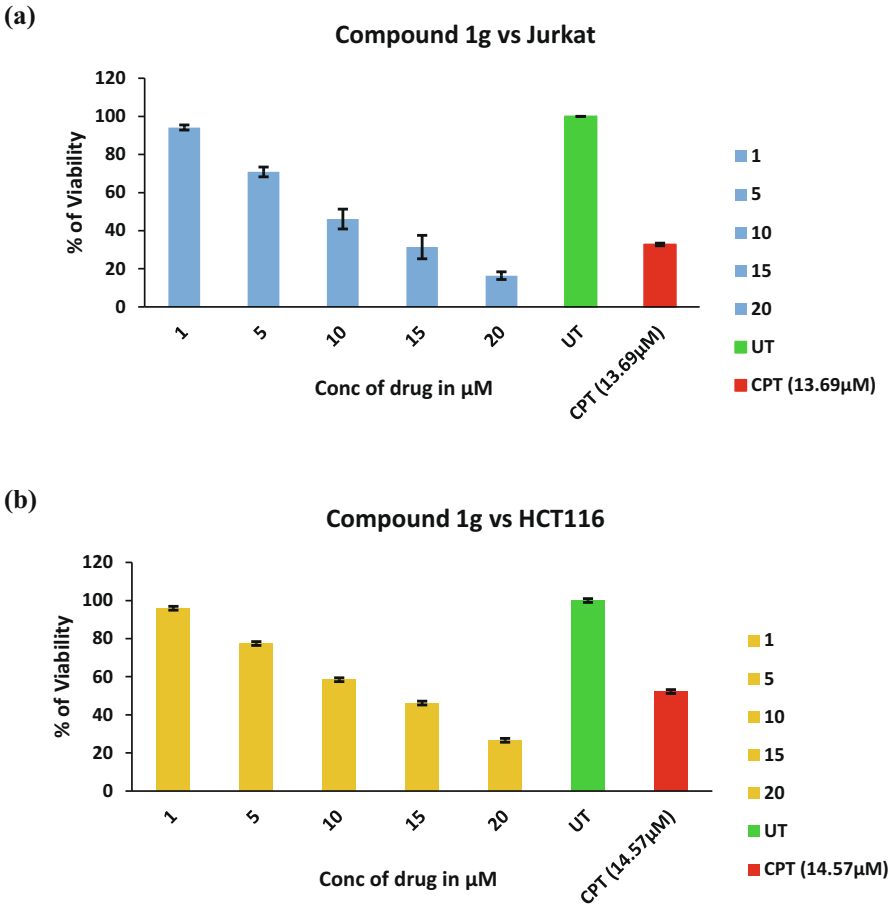


**Fig. 1.** Bar graphs representing % of cell viability after exposing to increasing concentrations of compound **1g** for 48 hrs. (a) % of JURKAT cell viability; (b) % of HCT116 cell viability.

**Table 1**
$IC_{50}$ value of synthesized analogous against HCT116 and JURKAT cell lines based on MTT antiproliferative activity assay.

| Entry | Compound | 24 hrs. treatment $IC_{50}$ values | | 48 hrs. treatment $IC_{50}$ values | |
|---|---|---|---|---|---|
| | | HCT116 | JURKAT | HCT116 | JURKAT |
| 1 | 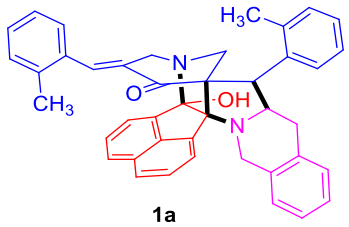 1a | 27.33 ± 1.13 | 64.66 ± 0.58 | NA | 34.55 ± 0.74 |
| 2 | 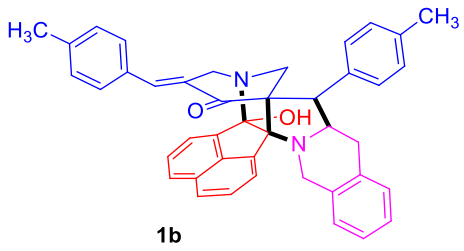 1b | 13.23 ± 0.56 | 72.35 ± 0.78 | 12.27 ± 1.11 | 30.11 ± 1.34 |
| 3 | 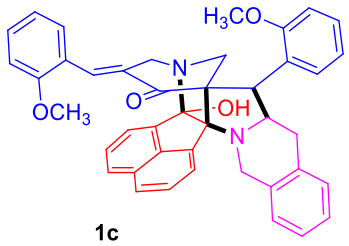 1c | 30.97 ± 1.31 | NA | 11.49 ± 0.89 | 67.29 ± 0.93 |
| 4 | 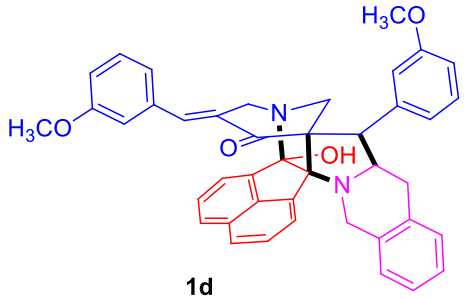 1d | 59.42 ± 1.37 | NA | 10.98 ± 0.73 | 63.6 ± 0.13 |
| 5 | 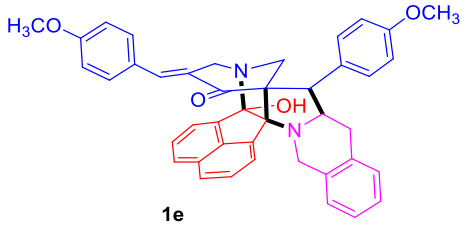 1e | NA | 120.52 ± 0.85 | NA | 64.35 ± 0.54 |
| 6 | 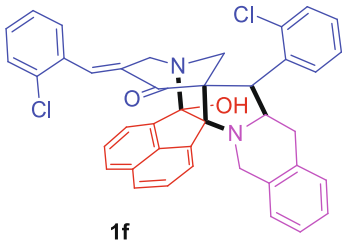 1f | 13.27 ± 0.64 | 14.64 ± 1.14 | NA | 10.68 ± 0.74 |

(*continued on next page*)

**Table 1** (*continued*)

| Entry | Compound | 24 hrs. treatment $IC_{50}$ values | | 48 hrs. treatment $IC_{50}$ values | |
|---|---|---|---|---|---|
| | | HCT116 | JURKAT | HCT116 | JURKAT |
| 7 | 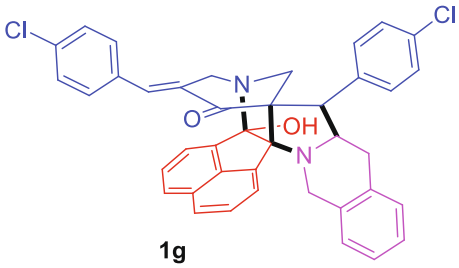 **1g** | 13.36 ± 0.83 | 15.75 ± 0.81 | 12.14 ± 1.53 | 10.68 ± 0.68 |
| 8 | 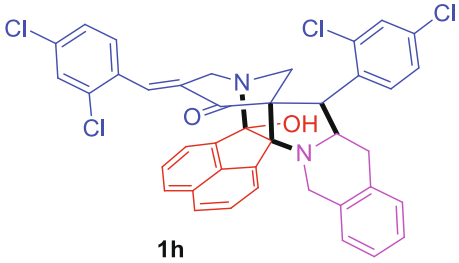 **1h** | NA | NA | NA | 71.69 ± 0.73 |
| 9 | 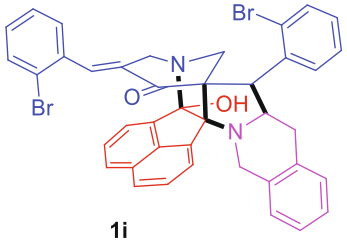 **1i** | 92.705 ± 0.66 | 15.03 ± 1.21 | NA | 10.70 ± 1.37 |
| 10 | 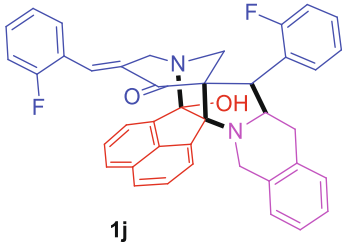 **1j** | 9.79 ± 0.73 | 15.61 ± 0.37 | 10.37 ± 0.88 | 10.17 ± 1.42 |
| 11 | 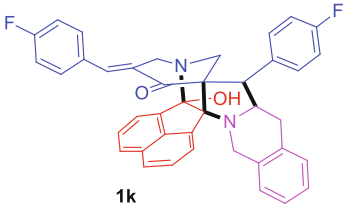 **1k** | 14.02 ± 1.11 | NA | 10.82 ± 0.83 | 68.21 ± 0.52 |
| 12 | 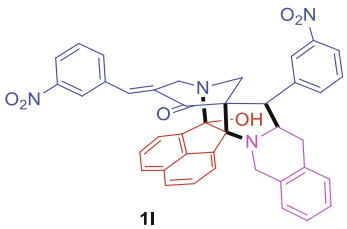 **1l** | 14.24 ± 0.74 | NA | 11.65 ± 1.04 | 69.48 ± 1.09 |
| 13 | CPT | 23.44 ± 0.81 | 18.33 ± 0.67 | 14.57 ± 0.43 | 13.69 ± 0.69 |

$IC_{50}$ values of test sample **1g**, positive control CPT respectively and the untreated cells were used as negative control. Post incubation of 48 hrs, the untreated cells and treated cells were washed twice with 1xPBS. The cells were then fixed and permeabilized with 70% ice cold ethanol at −20 °C for 30 min. These fixed cells were washed with PBS and resuspended with 50 µL of RNase A solution and 400 µL of Propidium Iodide solution (per million cells), vortexed and incubated for 10 min at RT. The cell cycle distribution in 10,000 cells was determined by flow cytometry.

*2.2.7. Statistical analysis*

The data are represented as the mean ± standard deviation (SD). SPSS software version 21.0 was used for the data analysis.

## 3. Results and discussion

### *3.1. Synthesis*

In the present study, a series of heterocyclic hybrids **1**(**a-l**) comprising biologically active pyrroloisoquinoline, pyridinone and acenaphthene structural units in a cage-like framework have been achieved (see Scheme 1) following the experimental procedure reported by us (Kumar et al., 2020). All the compounds were obtained in good to excellent yields and their structure was unambiguously derived using spectroscopic techniques. The synthesized cage-like heterocyclic hybrids **1**(**a-l**) were evaluated for their potential as anticancer agents.

### *3.2. Antiproliferative activity using MTT assay*

MTT assay is used as a sensitive, quantitative, and reliable colorimetric assay to measure viability, proliferation, and activation of cells. The MTT assay was performed to assess the $IC_{50}$ for synthesized compounds. Initially, synthesized compounds were evalu-

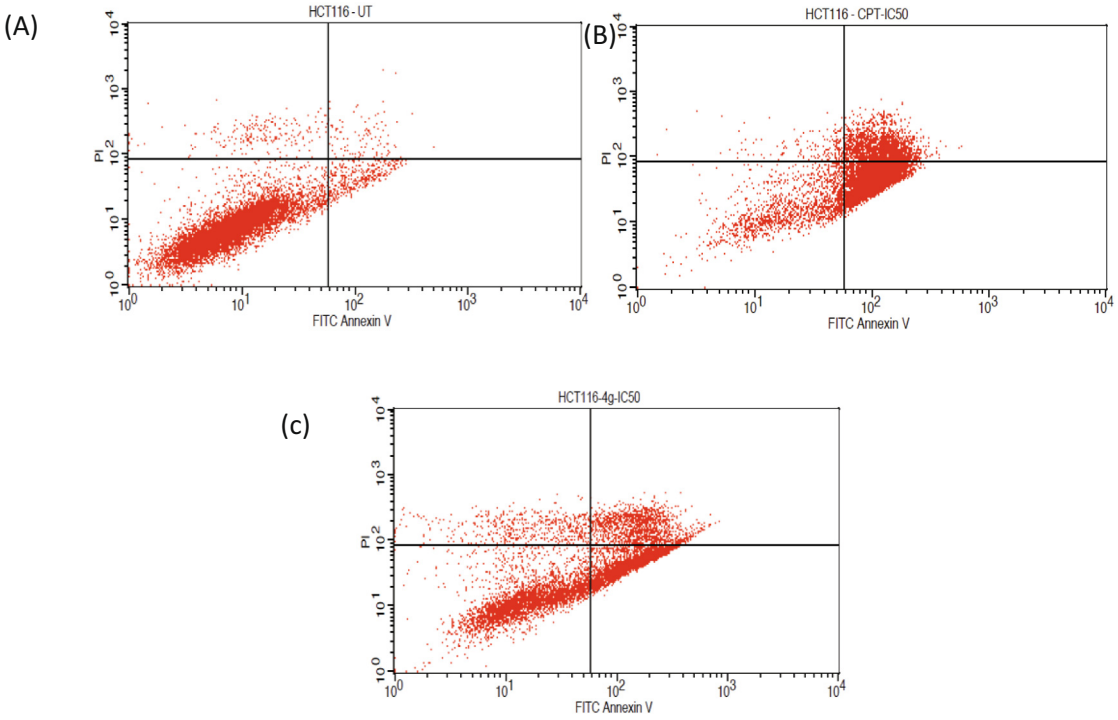


**Fig. 2.** Graph of FITC-Annexin V Vs PI staining against HCT-116 cell lines upon exposure with analogue **1g** and camptothecin at $IC_{50}$ value; (A) Control untreated HCT-116 cells; (B) HCT-116 Cells treated with standard drug camptothecin at $IC_{50}$ value; (C) HCT-116 cells treated with **1g** at $IC_{50}$ value.

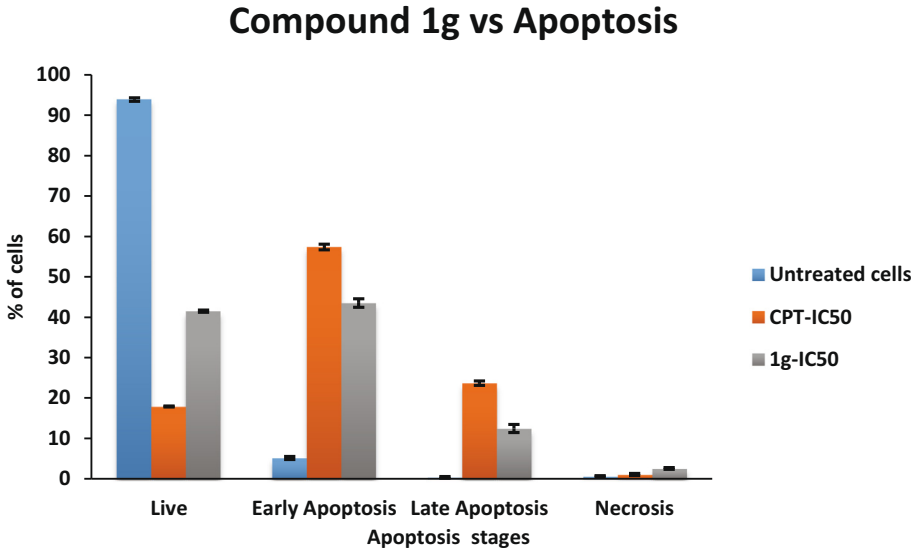


**Fig. 3.** Graph % of cells in each quadrant Vs compounds upon treatment with standard drug and analogue **1g**.

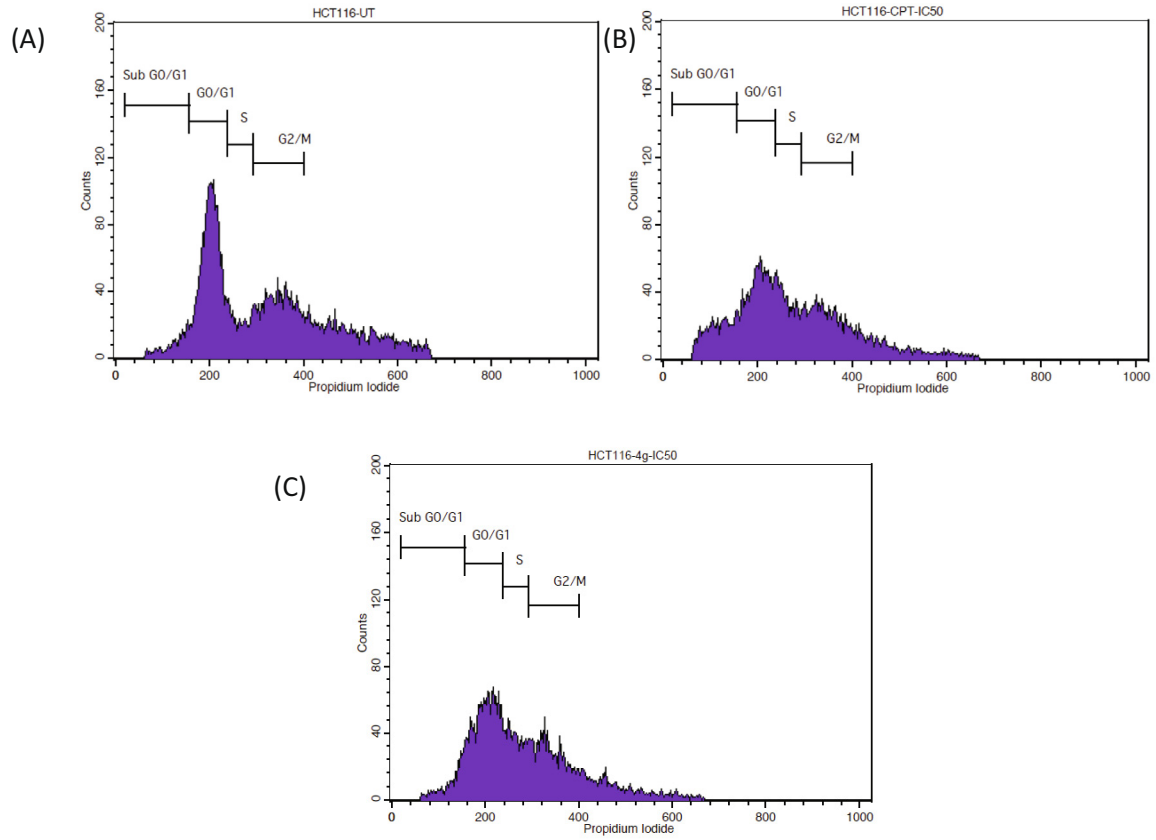


**Fig. 4.** FACS Histograms showing the phases of cell cycle distribution in the HCT-116 cell line treated with analogue **1g** and standard drug camptothecin at $IC_{50}$ value.

ated at 25, 50, 75, 100, 125 μM concentrations. At this concentration, all compounds exhibit significant and very potent activity against HCT-116 (colon cancer) and JURKAT (human T lymphocyte cells) cell lines. Based on significant activity, we further evaluated compounds at lower concentrations at 1, 5, 10, 15, and 20 μM concentration. Here, a dose-dependent reduction in the cell viability was detected upon treatment with various compounds. Here, camptothecin was used as standard drugs. From the entire datasets of twelve analogs, compound 1j exhibits potent activity against HCT-116 cell line with an $IC_{50}$ value of 10.37 μM, which was greater than standard compound camptothecin (14 μM) upon 48 hrs of the incubation time. Moreover, Compound **1g** exhibits potent activity on both HCT-116 and JURKAT cell lines with $IC_{50}$ values 12.14 and 10.68 μM, correspondingly (Fig. 1). The structure of all synthesized analogs along with $IC_{50}$ against HCT-116 and JURKAT cell lines are depicted in Table 1.

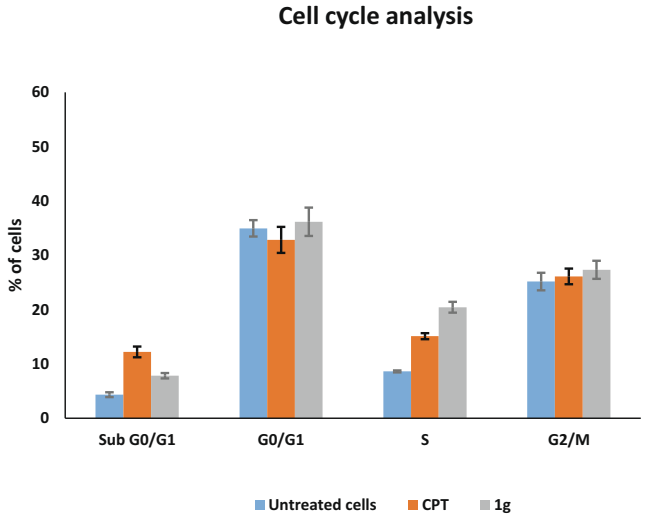


**Fig. 5.** Bar Plots of cell cycle phases of cells treated with CPT and its analogue **1g** at $IC_{50}$ value.

### 3.3. Apoptosis assay

To identify whether compound **1g** exhibits apoptosis, we performed apoptosis assay using Annexin V/FITC, and the fluorescence intensities of FITC-conjugated annexin-V and PI in cells and were analyzed using flow cytometry (Fig. 2). Apoptosis is the critical process for the death of the cancer cells. Upon exposure with compound **1g** at $IC_{50}$ value, 44.34% cells display early apoptosis and 14.52% cells display late apoptosis. The results indicated that compound **1g** significantly induces apoptosis in the HCT-116 cell lines (Fig. 3).

### 3.4. Cell cycle analysis

As shown in Fig. 4, cell cycle analysis of HCT-116 cells revealed that the cells treated with concentrations $IC_{50}$ of **1g** has high cells at the $G_0/G_1$ phase. The positive control, camptothecin (14 uM) shown the highest number of cells at the sub G0/G1 phase. There is no significant alteration observed amongst all the groups for the G2/M phase and S phase. Here, most active analogue **1g** and

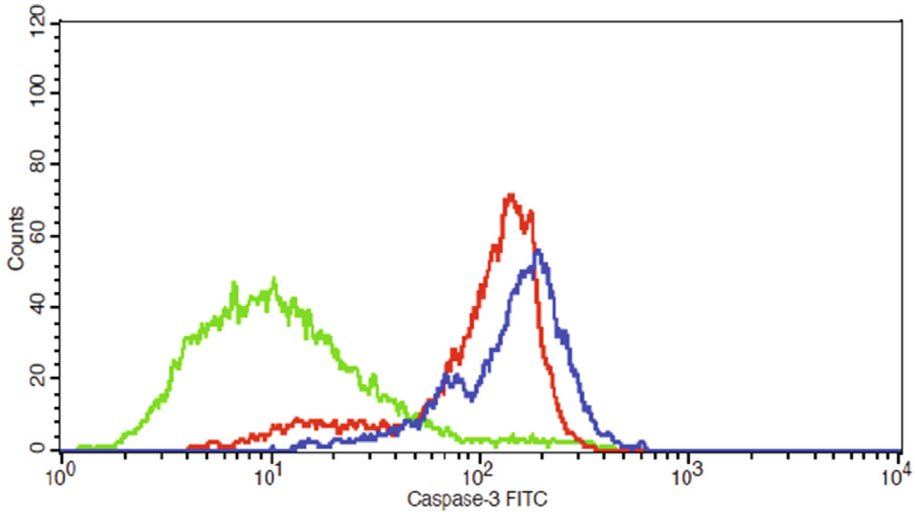


**Fig. 6.** Overlay of fluorescence intensities of caspase 3-FITC expression in HCT116 treated with IC50 values of **1g** and CPT for 48 hr.

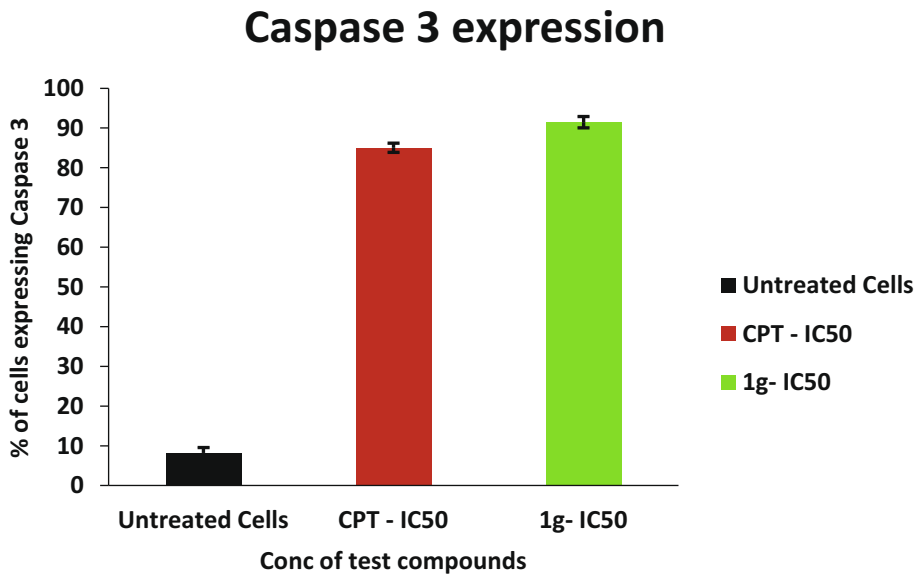


**Fig. 7.** Graph depicting the Caspase 3 quantification in HCT-116 cells treated with analogue **1g** and positive control camptothecin.

camptothecin follows similar pattern in cell cycle upon treatment at $IC_{50}$ concentration (Fig. 5).

### 3.5. Caspase 3 induction assay

Caspase 3 was up-regulated, as shown in Fig. 6. Analogue **1g** shown the highest induction of caspase 3 while there was the lowest expression in solvent treated cells (negative control). The results suggest that as analogue **1g** exhibits significant caspase 3 induction which is also higher than standard drug camptothecin upon treatment with $IC_{50}$ concentration (Fig. 7).

### 3.6. Assessment of mitochondrial membrane potential ($\Delta\Psi$ m)

Mitochondria are related to apoptosis initiation and progression. Disturbance in MMP can release proapoptotic factors, such as cytochrome c and apoptosis-inducing factor. During apoptosis, the collapse of the MMP coincides with the opening of the mitochondrial permeability transition pores, leading to the release of cytochrome c into the cytosol, which in turn triggers other downstream events in the apoptotic cascade. Upon exposure with analogue **1g** and camptothecin increase in mitochondrial membrane potential was observed (Figs. 8 and 9).

### 3.7. TUNEL assay

TUNEL is a method for evaluation of apoptotic DNA fragmentation, widely used to identify and quantify apoptotic cells, or to detect excessive DNA breakage in individual cells. Here, upon treatment with analogue **1g** and camptothecin; **1g** treated cells show greater number of apoptotic cells as compare to control cells (Figs. 10 and 11).

## 4. Conclusions

A small library of cage-like heterocyclic hybrids **1(a-l)** encompassing biologically active pyrroloisoquinolines, pyridinone and acenaphthene structural moieties have been synthesized and

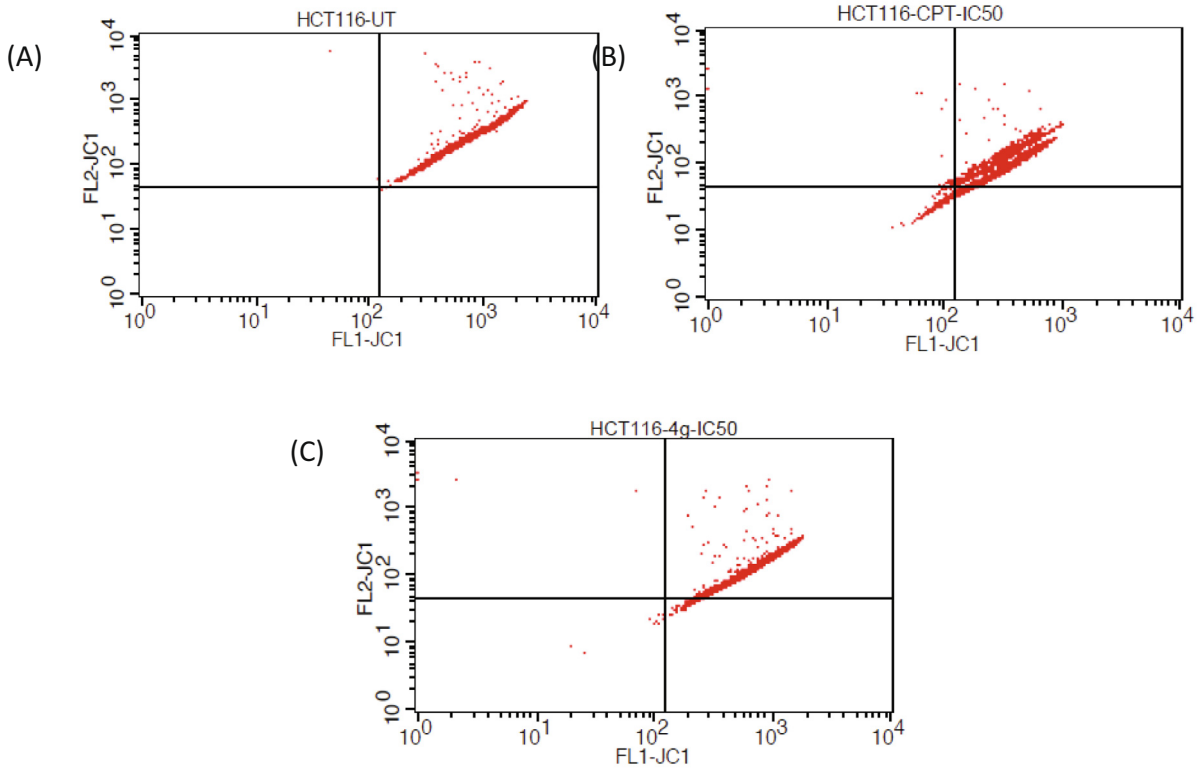


**Fig. 8.** Graph of FLT-JC1 Vs FLT-JC2 against HCT-116 cell lines upon exposure with analogue **1g** and camptothecin at $IC_{50}$ value; (A) Control untreated HCT-116 cells; (B) HCT-116 Cells treated with standard drug camptothecin at $IC_{50}$ value; (C) HCT-116 Cells treated with 4 g at $IC_{50}$ value.

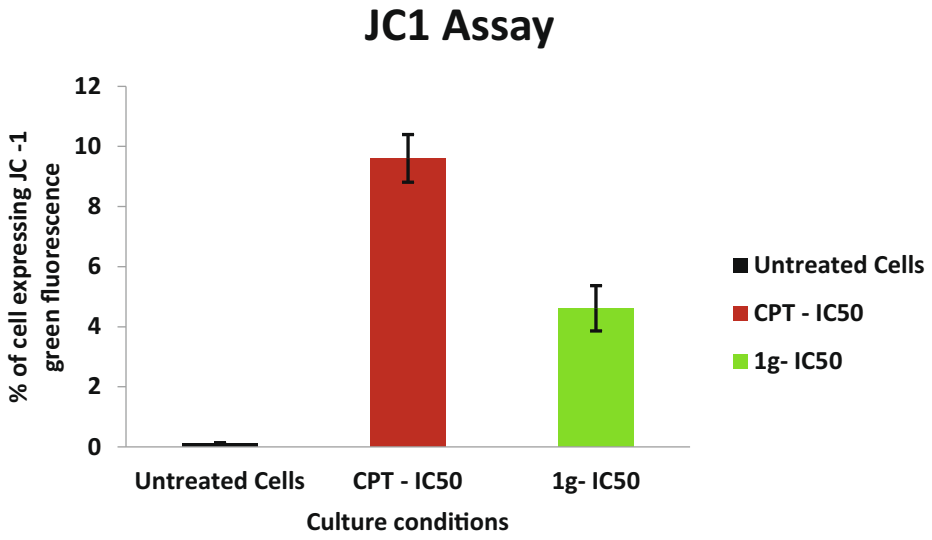


**Fig. 9.** Graph depicting the JC1 quantification in HCT-116 cells treated with analogue **1g** and positive control camptothecin.

tested for their potential as anticancer agents against HCT116 and JURKAT cell lines. The analogues exhibit dose dependent reduction with significant anticancer activity. The results of MTT assay reveals that analogue **1g** able to inhibit HCT-116 (colon cancer cell line) and JURKAT cell line with $IC_{50}$ values 12.14 and 10.68 μM individually. Based on excellent inhibitory activity in MTT assay, analogue **1g** was further evaluated for apoptosis and cell cycle analysis. The results suggest that analogue **1g** able to induce apoptosis at early stage in HCT-116 cell line and also arrest cell line which is equivalent to standard drug camptothecin. Further, analogue **1g** also increase threshold of MMP which is important for apoptosis of cancer cells. The results of *in vitro* anticancer activity strongly indicate that **1g** may become a potential molecule to develop as drug candidate.

## Declaration of Competing Interest

The authors declare that they have no known competing financial interests or personal relationships that could have appeared to influence the work reported in this paper.

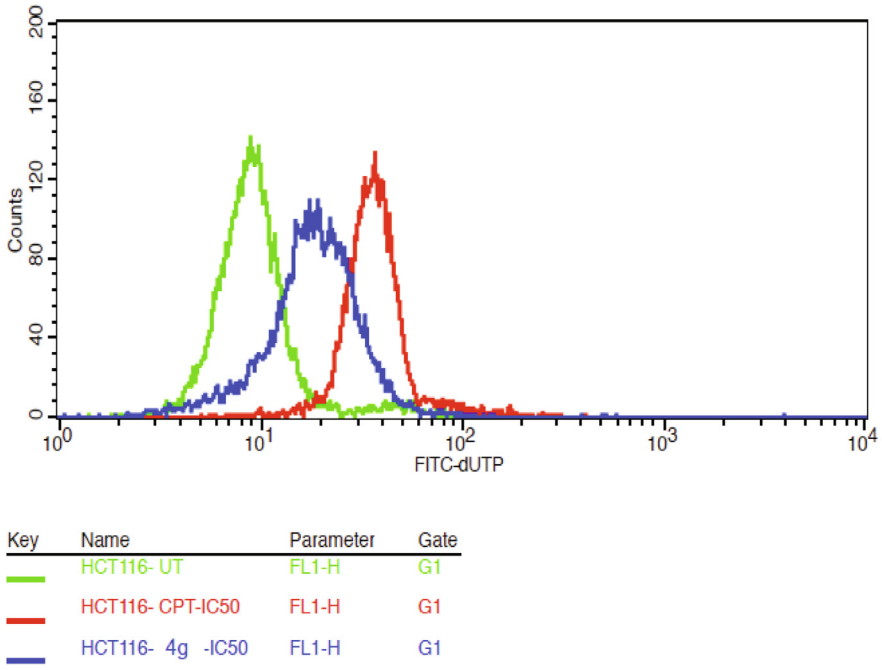


**Fig. 10.** Overlay of fluorescence intensities of FITC-dUTP expression in HCT116 treated with IC50 values of **1g** and CPT for 48 hr.

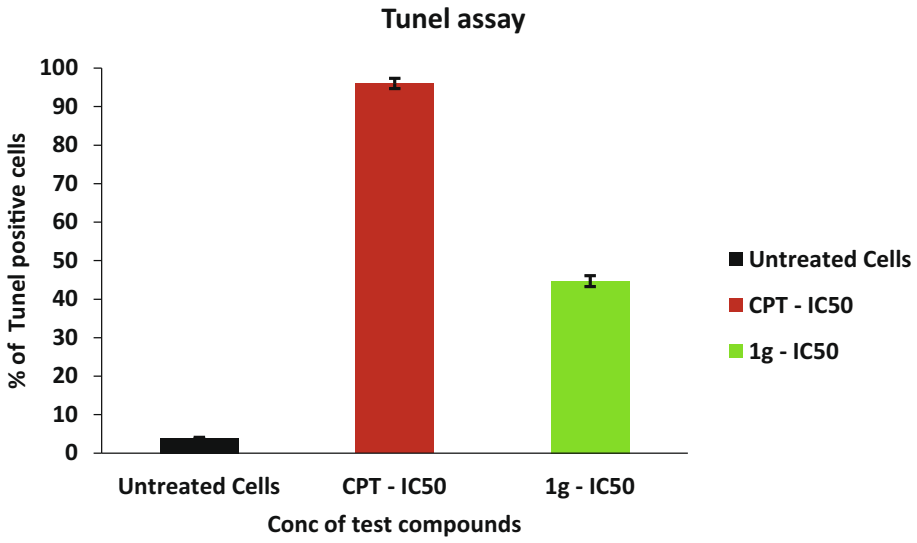


**Fig. 11.** Graph of FITC-dUTP Vs Count against HCT-116 cell lines upon treatment with analogue **1g** and camptothecin at $IC_{50}$ value.

## Acknowledgments

The project was supported by Researchers Supporting Project number (RSP-2020/231), King Saud University, Riyadh, Saudi Arabia.

## References

Adrouny, A.R., 2002. Understanding Colon Cancer. Univ. Press of Mississippi.
Ames, B.N., Gold, L.S., Willett, W.C., 1995. The causes and prevention of cancer. Proc. Natl. Acad. Sci. 92, 5258–5265.
Andreev, I.A., Ratmanova, N.K., Novoselov, A.M., Belov, D.S., Seregina, I.F., Kurkin, A. V., 2016. Oxidative dearomatization of 4,5,6,7-tetrahydro-1H-indoles obtained by metal- and solvent-free thermal 5-endo-dig cyclization: the route to erythrina and lycorine alkaloids. Chem. – Eur. J. 22, 7262–7267.
Boyle, P., Maisonneuve, P., Autier, P., 2000. Update on cancer control in women. Int. J. Gynecol. Obstet. 70, 263–303.
Chakraborty, I., Jana, S., 2013. Synthetic developments on the indolizidine alkaloid, harmicine. Synthesis 45, 3325–3331.
Chen, Q., Xu, L., Liang, C., Wang, C., Peng, R., Liu, Z., 2016. Photothermal therapy with immune-adjuvant nanoparticles together with checkpoint blockade for effective cancer immunotherapy. Nat. Commun. 7, 1–3.
Eicher, T., Hauptmann, S., Speicher, A. (Eds.), 2012. The Chemistry of Heterocycles: Structure, Reactions, Synthesis, and Applications. third ed. Wiley-VCH, Weinheim, Germany.
Gomtsyan, A., 2012. Heterocycles in drugs and drug discovery. Chem. Heterocycl. Compd. 48, 7–10.
Gralow, J., Ozols, R.F., Bajorin, D.F., Cheson, B.D., Sandler, H.M., Winer, E.P., Bonner, J., Demetri, G.D., Curran, W., Ganz, P.A., Kramer, B.S., 2008. Clinical cancer advances 2007: major research advances in cancer treatment, prevention, and

screening-a report from the American Society of Clinical Oncology. J. Clin. Oncol. 26, 313–325.
Grossman, S.A., Batara, J.F., 2004. Current management of glioblastoma multiforme. In: Seminars in Oncology, vol. 31, no. 5, pp. 635–644. WB Saunders.
Kam, T.-S., Sim, K.-W., 1998. Alkaloids from *Kopsia griffithii*. Phytochemistry 47, 145–147.
Kanavos, P., 2006. The rising burden of cancer in the developing world. Ann. Oncol. 17 (suppl_8), viii15–viii23.
Kumar, R.S., Almansour, A.I., Arumugam, N., 2020. In vitro mechanistic investigation of polycyclic cage-like heterocyclic hybrid possessing diverse pharmacophoric units. J. King Saud Univ. Sci. 32, 2406–2413.
Lim, D.R., Kuk, J.K., Kim, T., Shin, E.J., 2017. Comparison of oncological outcomes of right-sided colon cancer versus left-sided colon cancer after curative resection: Which side is better outcome?. Medicine 96, 42.
Liu, F., Qian, X., Cui, J., Xiao, Y., Zhang, R., Li, G., 2006. Design, synthesis, and antitumor evaluation of novel acenaphtho[1,2-b]pyrrole-carboxylic acid esters with amino chain substitution. Bioorg. Med. Chem. 14, 4639–4644.
Maier-Hauff, K., Rothe, R., Scholz, R., Gneveckow, U., Wust, P., Thiesen, B., Feussner, A., von Deimling, A., Waldoefner, N., Felix, R., Jordan, A., 2007. Intracranial thermotherapy using magnetic nanoparticles combined with external beam radiotherapy: results of a feasibility study on patients with glioblastoma multiforme. J. Neurooncol. 81, 53–60.
Nair, J.J., van Staden, J., Bastida, J., 2016. Apoptosis-inducing effects of amaryllidaceae alkaloids. Curr. Med. Chem. 23, 161–185.
Pereira, M.F., Rochais, C., Dallemagne, P., 2015. Recent advances in phenanthroindolizidine and phenanthroquinolizidine derivatives with anticancer activities. AntiCancer Agents Med. Chem. 15, 1080–1081.
Santiago-Vazquez, Y., Das, S., Das, U., Robles-Escajeda, E., Ortega, N.M., Lema, C., Varela-Ramírez, A., Aguilera, R.J., Balzarini, J., De Clercq, E., Dimmock, S.G., Gorecki, D.K., Dimmock, J.R., 2014. Novel 3,5-bis(arylidene)-4-oxo-1-piperidinyl dimers: structure-activity relationships and potent antileukemic and antilymphoma cytotoxicity. Eur. J. Med. Chem. 77, 315–322.
Sorgi, K.L., Maryanoff, C.A., McComsey, D.F., Graden, D.W., Maryanoff, B.E., 1990. Asymmetric induction in an enammonium-iminium rearrangement. Mechanistic insight via NMR, deuterium labeling, and reaction rate studies. Application to the stereoselective synthesis of pyrroloisoquinoline antidepressants. J. Am. Chem. Soc. 112, 3567–3579.
Stewart, B.W., Kleihues, P. (Eds.), 2014. World Cancer Report.
Todaro, M., Alea, M.P., Di Stefano, A.B., Cammareri, P., Vermeulen, L., Iovino, F., Tripodo, C., Russo, A., Gulotta, G., Medema, J.P., Stassi, G., 2007. Colon cancer stem cells dictate tumor growth and resist cell death by production of interleukin-4. Cell Stem Cell 1, 389–402.
Weidner, N., 1995. Current pathologic methods for measuring intratumoral microvessel density within breast carcinoma and other solid tumors. Breast Cancer Res. Treat. 36, 169–180.
Wolinsky, J.B., Colson, Y.L., Grinstaff, M.W., 2012. Local drug delivery strategies for cancer treatment: gels, nanoparticles, polymeric films, rods, and wafers. J Control Release. 159, 14–26.
Zhang, Q., Tu, G., Zhao, Y., Cheng, T., 2002. Novel bioactive isoquinoline alkaloids from *Carduus crispus*. Tetrahedron 58, 6795–6798.
Zhang, Z., Yang, Y., Zhang, D., Wang, Y., Qian, X., Liu, F., 2006. Acenaphtho[1,2-b] pyrrole derivatives as new family of intercalators: various DNA binding geometry and interesting antitumor capacity. Bioorg. Med. Chem. 14, 6962–6970.